ORIGINAL INVESTIGATION

Assessing the predicted impact of single amino acid substitutions in calmodulin for CAGI6 challenges

Paola Turina[1] · Giuditta Dal Cortivo[2] · Carlos A. Enriquez Sandoval[1] · Emil Alexov[3] · David B. Ascher[4,5] ·
Giulia Babbi[1] · Constantina Bakolitsa[6] · Rita Casadio[1] · Piero Fariselli[7] · Lukas Folkman[8] · Akash Kamandula[9] ·
Panagiotis Katsonis[10] · Dong Li[11] · Olivier Lichtarge[10] · Pier Luigi Martelli[1] · Shailesh Kumar Panday[3] ·
Douglas E. V. Pires[12] · Stephanie Portelli[4,5] · Fabrizio Pucci[11] · Carlos H. M. Rodrigues[4] · Marianne Rooman[11] ·
Castrense Savojardo[1] · Martin Schwersensky[11] · Yang Shen[13] · Alexey V. Strokach[14] · Yuanfei Sun[13] · Junwoo Woo[15] ·
Predrag Radivojac[9] · Steven E. Brenner[6,16,17] · Daniele Dell'Orco[2] · Emidio Capriotti[1,18]

Abstract

Recent thermodynamic and functional studies have been conducted to evaluate the impact of amino acid substitutions on Calmodulin (CaM). The Critical Assessment of Genome Interpretation (CAGI) data provider at University of Verona (Italy) measured the melting temperature (T_m) and the percentage of unfolding (%unfold) of a set of CaM variants (CaM challenge dataset). Thermodynamic measurements for the equilibrium unfolding of CaM were obtained by monitoring far-UV Circular Dichroism as a function of temperature. These measurements were used to determine the T_m and the percentage of protein remaining unfolded at the highest temperature. The CaM challenge dataset, comprising a total of 15 single amino acid substitutions, was used to evaluate the effectiveness of computational methods in predicting the T_m and unfolding percentages associated with the variants, and categorizing them as destabilizing or not. For the sixth edition of CAGI, nine independent research groups from four continents (Asia, Australia, Europe, and North America) submitted over 52 sets of predictions, derived from various approaches. In this manuscript, we summarize the results of our assessment to highlight the potential limitations of current algorithms and provide insights into the future development of more accurate prediction tools. By evaluating the thermodynamic stability of CaM variants, this study aims to enhance our understanding of the relationship between amino acid substitutions and protein stability, ultimately contributing to more accurate predictions of the effects of genetic variants.

Introduction

Calmodulin (CaM) is a 149 amino acid long, highly conserved, ubiquitous calcium-binding messenger protein, found in all eukaryotic cells. Its structure is composed of two lobes, with each lobe containing two EF-hand motifs, connected by a flexible linker, capable of binding calcium ions (Ca^{2+}) and several targets (Radivojac et al. 2006). It plays a pivotal role in transducing calcium signals by binding Ca^{2+} and subsequently interacting with various target proteins, thereby modulating numerous cellular processes (Chin and Means 2000). These processes include muscle contraction, cell division, signal transduction pathways,

making calmodulin extensively involved in cellular homeostasis and function (Clapham 2007). The C-terminal domain of CaM, constituted by the EF3 and EF4 motifs, binds Ca^{2+} with higher affinity ($K_d \sim 1\ \mu M$) than the N-terminal domain formed by EF1 and EF2 ($K_d \sim 10\ \mu M$) (Linse et al. 1991). Ca^{2+} binding to each globular domain leads to substantial alterations in the packing of the EF-hands, resulting in a more open conformation as compared to the closed conformation observed in the absence of Ca^{2+}, where the helices in the two lobes are packed against each other, with most of the hydrophobic residues shielded from the solvent. (Zhang et al. 1995). The exposure of hydrophobic sites following Ca^{2+} binding constitutes the prerequisite for the high structural and functional plasticity of CaM, which enables the protein to bind to and activate many target proteins. Furthermore, the fact that Ca^{2+} binding occurs with positive cooperativity within each domain and that CaM can recognize its

Paola Turina and Giuditta Dal Cortivo have Co-first authors.

Extended author information available on the last page of the article

molecular target even in the absence of Ca^{2+} creates a strong coupling between the free energy of Ca^{2+} binding and that of the target, with important consequences for the stability of its folding (Valeyev et al. 2008).

Given CaM's ample spectrum of binding partners across so many physiological processes (Hoeflich and Ikura 2002), any impairment in its function may be associated with a variety of pathological conditions. Dysregulation of CaM-mediated pathways has been linked to cancer (Nussinov et al. 2017), cardiovascular diseases (Beghi et al. 2022) and neurodegenerative disorders (Bohush et al. 2021). Its structure enables CaM to undergo significant conformational changes upon calcium binding, featuring a conformational flexibility which allows CaM to interact with a variety of target proteins, thus exerting its regulatory activity in many cellular processes (Crivici and Ikura 1995). Recent studies have revealed that CaM can exhibit distinct conformational states and interaction modes depending on its binding partners and cellular context (Tidow and Nissen 2013). Several mutations in the primary sequence of CaM are known, which can significantly impact on its function. These mutations, particularly in the EF-hand motifs, can alter calcium binding affinity, conformational dynamics, and interactions with target proteins, leading to various disease phenotypes (Hussey et al. 2023). Investigating the biochemical and biophysical properties of wild-type and mutant calmodulin is needed for understanding the molecular basis of their pathological consequences. One prominent molecular property in evaluating the pathogenicity of a mutant is its eventual effect on the protein thermodynamic stability (Gerasimavicius et al. 2020; Birolo et al. 2021). A change in the latter is estimated to represent a major pathogenicity effector in a large proportion of disease-related single-site missense mutations in the whole human proteome, making thermodynamic stability change one of the most important parameters to be evaluated when investigating the molecular basis of a disease (Stein et al. 2019; Petrosino et al. 2021). In the past, a variety of algorithms have been developed to predict how amino acid substitutions affect the protein folding free energy (Marabotti et al. 2021). Such prediction tools utilize a range of methodologies, including empirical energy functions and machine learning-based approaches (Compiani and Capriotti 2013). In spite of the fact that the performance of those predictive methods has reached a considerable level in the past few years, major issues remain in their evaluation, standardization, and further improvement possibilities (Sanavia et al. 2020; Pancotti et al. 2022).

To address these issues, the previous edition of the Critical Assessment of Genome Interpretation (CAGI) introduced a challenge focused on predicting the impact of eight single amino acid variants on the stability of the human frataxin protein (Savojardo et al. 2019; Petrosino et al. 2019; Critical Assessment of Genome Interpretation Consortium 2024).

Building on this effort, and based on a previous CAGI challenge focusing on the functional impact of missense mutation on calmodulin (Zhang et al. 2019), the sixth edition of the CAGI experiments presented a new challenge, aimed to evaluate the performance of computational methods in predicting the measured stability changes for 15 single amino acid variants in CaM in terms of melting temperature (T_m) and percentage of unfolding.

Materials and methods

Experimental measures

Human CaM protein (reference UniProt ID: P0DP23 for gene CALM1; equivalent to P0DP24 and P0DP25 for genes CALM2 and CALM3) and its variants were expressed in *E. coli* cells, and purified by reverse immobilized metal affinity chromatography (Dal Cortivo et al. 2022). Equilibrium unfolding of both wild-type and variant CaM proteins was achieved by incubating them at increasing temperatures, from 4 to 120 °C. Circular dichroism (CD) spectra were recorded for all proteins as described (Dal Cortivo et al. 2023). Melting temperatures (T_m) were determined from the first derivative of the ellipticity changes at 222 nm. The analysis of spectral changes in far-UV CD ellipticity involved fitting data to a thermodynamic or to an empirical function. Furthermore, the ellipticity values at 222 nm, measured at 4 °C and 120 °C, were used to calculate the percentage of unfolded structure of the protein (%unfold). Measurements were carried out for both the apo (no bound Ca^{2+}) and holo (bound Ca^{2+}) forms. The CaM protein was incubated with EGTA for the apo form and with 300 µM Ca^{2+} for the holo form, followed by recording their respective CD spectra under the same conditions. This allowed for the comparison of structural stability and unfolding characteristics between the apo and holo states of CaM proteins and their variants. Further details on the experimental techniques and data analysis procedures are provided in (Dal Cortivo et al. 2023).

CaM challenge dataset

The CaM challenge dataset, organized in the CAGI6, consisted of 15 coding variants potentially associated with sudden heart failure (Jensen et al. 2018). A representation of the mutated sites in the three-dimensional structures of the CaM apo (PDB: 1DMO) and holo (PDB: 1CLL) forms are displayed in Fig. 1.

To evaluate the effect of the amino acid substitution on protein stability, the thermal denaturation (TD) profiles of the calmodulin variants were collected, using three technical replicates. A polynomial function was fitted to the TD profiles to determine the melting temperature (T_m),
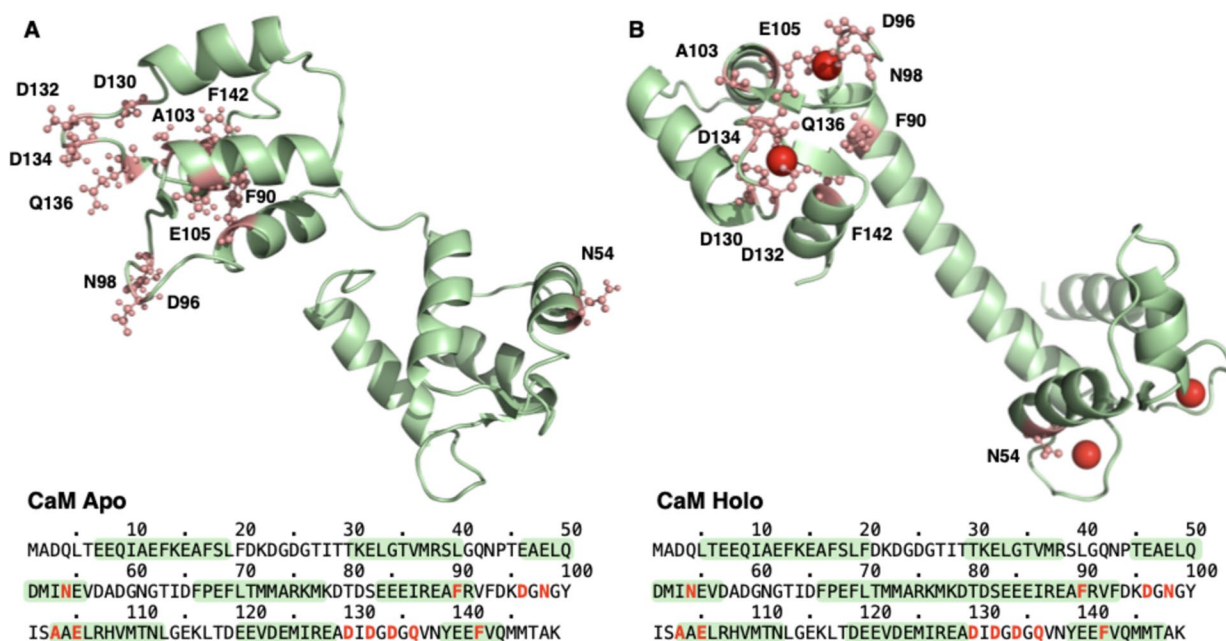
Fig. 1 Mapping of the 11 mutated sites corresponding to the 16 mutations from the CaM challenge dataset (shown in red) on the three-dimensional structures of calmodulin in its apo (**A**) and holo (**B**) forms. The structures for the apo and holo forms are derived from PDB entries 1DMO and 1CLL, respectively. In **A**, the variant aspar-agine in position 130, present in the original 1DMO structure, was replaced with the wild-type aspartic acid. In **B** the red spheres represent the Ca^{2+} ions. The experimental data of the p.F142L variant was excluded from the assessment, as it was released after the end of the challenge

identified at the zeros of the second derivative of the polynomial function, where the first derivative showed local maxima. This fitting procedure was consistently applied to all CaM variants in both the apo and the holo forms, using the same polynomial function for all profiles. Additionally, TD profiles were fitted with the following equation describing a thermodynamic model of a two-state unfolding process,

$$\theta_{222}(T) = \frac{(b_f + k_f T) + (b_u + k_u T \exp[-\Delta G_{fu}(T)])}{1 + \exp[-\Delta G_{fu}(T)/RT]} \quad (1)$$

where the b and k are the baselines and slopes of the folded (f) and unfolded (u) states, ΔG_{fu} Gibbs free energy, and T the temperature.

The percentage of unfolding (%unfold) at 120 °C was calculated based on ellipticity values at 222 nm recorded at 4 °C (θ_{222}^4) and 120 °C (θ_{222}^{120}) as follows:

$$\%unfold = \frac{\theta_{222}^{120} - \theta_{222}^4}{\theta_{222}^4} \quad (2)$$

The final set of variants with the relative average of T_m and the %unfold obtained from three technical replicates and their experimental errors, for both the apo and holo forms of CaM, are reported in Tables 1 and 2 respectively. A comparison of the T_m and %unfold values for the apo

Table 1 Experimental unfolding data of the apo form of calmodulin (Ca^{2+} free)

Protein	T_m (°C)	ΔT_m (°C)	%unfold	Δ%unfold
Wild-type	59.2 ± 0.2	–	71.8 ± 0.4	–
p.N54I	55.6 ± 0.7	− 3.6 ± 0.7	72.8 ± 0.9	− 1.0 ± 1.0
p.F90L	60.2 ± 1.0	1.0 ± 1.0	71.2 ± 2.5	0.6 ± 2.5
p.D96H	59.2 ± 0.4	0.0 ± 0.4	72.4 ± 1.1	− 0.6 ± 1.2
p.D96V	58.7 ± 0.4	− 0.5 ± 0.4	71.9 ± 0.3	− 0.1 ± 0.5
p.N98I	59.7 ± 0.3	0.5 ± 0.4	72.2 ± 0.4	− 0.4 ± 0.6
p.N98S	60.5 ± 0.4	1.3 ± 0.4	77.2 ± 1.7	− 5.4 ± 1.7
p.A103V	60.8 ± 0.3	1.6 ± 0.4	72.7 ± 0.4	− 0.9 ± 0.6
p.E105A	59.4 ± 0.6	0.2 ± 0.6	72.0 ± 0.3	− 0.2 ± 0.5
p.D130G	61.2 ± 0.2	2.0 ± 0.3	73.6 ± 0.6	− 1.8 ± 0.7
p.D130V	59.7 ± 0.6	0.5 ± 0.6	70.8 ± 1.1	1.0 ± 1.2
p.D132E	59.4 ± 0.4	0.2 ± 0.4	73.6 ± 0.7	− 1.8 ± 0.8
p.D132H	59.7 ± 0.6	0.5 ± 0.6	73.5 ± 0.5	− 1.7 ± 0.6
p.D132V	60.0 ± 0.3	0.8 ± 0.4	72.9 ± 0.3	− 1.1 ± 0.5
p.D134H	59.5 ± 0.2	0.3 ± 0.3	73.1 ± 1.0	− 1.3 ± 1.1
p.Q136P	59.6 ± 0.8	0.4 ± 0.8	73.1 ± 0.8	− 1.3 ± 0.9
p.F142L*	62.1 ± 0.5	2.9 ± 0.5	72.8 ± 1.2	− 1.0 ± 1.3

T_m = melting temperature. *%unfold* = percentage of unfolded protein at 120 °C. $\Delta T_m = T_m^{mut} - T_m^{wt}$. Δ%unfold = %unfold^{wt} − %unfold^{mut}.

*The experimental data for the p.F142L variant was excluded from the assessment, as it was released after the end of the challenge

Table 2 Experimental unfolding data of the holo form of calmodulin (Ca^{2+} bounded)

Protein	T_m (ºC)	ΔT_m (ºC)	%unfold	Δ%unfold
Wild-type	109.1 ± 1.2	–	74.8 ± 0.6	–
p.N54I	109.7 ± 0.4	0.6 ± 1.3	75.0 ± 0.4	-0.2 ± 0.7
p.F90L	103.4 ± 1.5	-5.7 ± 1.9	75.7 ± 1.3	-0.9 ± 1.4
p.D96H	103.3 ± 0.7	-5.8 ± 1.4	75.3 ± 0.6	-0.5 ± 0.8
p.D96V	103.3 ± 1.7	-5.8 ± 2.1	75.1 ± 1.2	-0.3 ± 1.3
p.N98I	103.3 ± 0.7	-5.8 ± 1.4	75.3 ± 1.1	-0.5 ± 1.3
p.N98S	105.9 ± 0.6	-3.2 ± 1.3	76.1 ± 0.4	-1.3 ± 0.7
p.A103V	107.3 ± 0.6	-1.8 ± 1.3	76.1 ± 0.2	-1.3 ± 0.6
p.E105A	102.9 ± 0.5	-6.2 ± 1.3	74.1 ± 1.1	0.7 ± 1.3
p.D130G	103.3 ± 1.3	-5.8 ± 1.8	73.8 ± 0.2	1.0 ± 0.6
p.D130V	103.6 ± 0.5	-5.5 ± 1.3	73.8 ± 5.8	1.0 ± 5.8
p.D132E	103.4 ± 2.1	-5.7 ± 2.4	73.6 ± 1.2	1.2 ± 1.3
p.D132H	104.1 ± 0.9	-5.0 ± 1.5	72.2 ± 0.8	2.6 ± 1.0
p.D132V	105.9 ± 1.1	-3.2 ± 1.6	75.8 ± 0.7	-1.0 ± 0.9
p.D134H	103.2 ± 0.6	-5.9 ± 1.3	70.8 ± 1.4	4.0 ± 1.5
p.Q136P	103.6 ± 0.9	-5.5 ± 1.5	67.1 ± 0.6	7.7 ± 0.8
p.F142L*	106.5 ± 0.4	-2.6 ± 1.3	75.2 ± 0.6	-0.4 ± 0.8

T_m = melting temperature. %*unfold* = percentage of unfolded protein at 120 ºC. $\Delta T_m = T_m^{mut} - T_m^{wt}$. Δ%unfold = %unfold^{wt} − %unfold^{mut}.

*The experimental data for the p.F142L variant was excluded from the assessment, as it was released after the end of the challenge

and holo forms of CaM, and their differences relative to the wild-type, is shown in Fig. S1 and Fig. 2, respectively.

Challenge participants and prediction methods

Nine groups participated in the CAGI6 CaM challenge, collectively submitting 52 sets of predictions. Of these, 20 sets were for the apo form and 19 sets for the holo form, while the remaining 13 sets were compared against data for both the apo and holo forms of calmodulin. Here, we provide a brief description of the prediction sets submitted by the participating teams.

Team 1: The *3billion* team used the 3Cnet algorithm (Won et al. 2021), training on 73,822 missense mutations from the ClinVar database (Landrum et al. 2020). They distinguished between pathogenic and benign variants and supplemented their data with common benign variants from the gnomAD database (Karczewski et al. 2020). Conservation data was generated through multiple sequence alignment (MSA) across 53,998 transcripts. Their prediction method involved bidirectional LSTM networks for feature extraction and a pathogenicity classifier, followed by mapping scores to thermodynamic stability values for "Stabilizing-vs-Destabilizing" predictions.

Team 2: The *AIBI-CAGI6* team pre-trained protein language models, like BERT, on domain sequences from the Pfam database (Sun and Shen 2024). They opti-
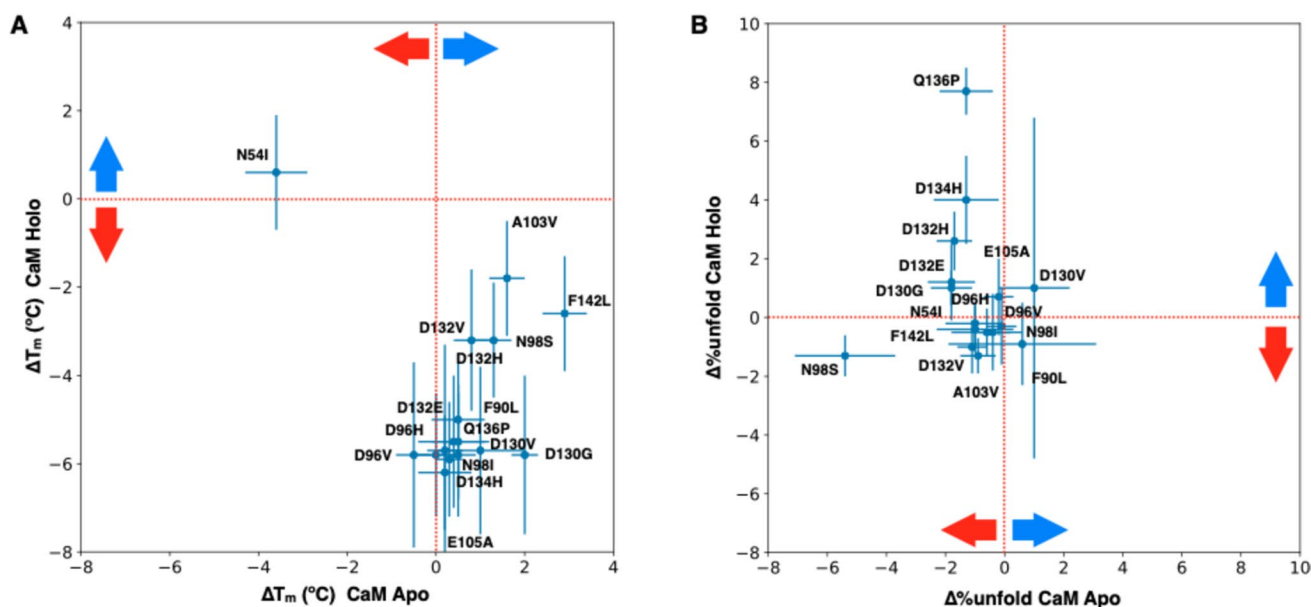
Fig. 2 Comparison of the changes in melting temperature (**A**) and %unfold (**B**) for the apo and holo forms of calmodulin. The change in melting temperature (ΔT_m, panel **A**) is calculated as $\Delta T_m = T_m^{mut} - T_m^{wt}$. **B** Shows the change in %unfold (Δ%unfold), calculated as %unfold^{wt} − %unfold^{mut} to maintain consistency in sign. Variants are considered stabilizing if their ΔT_m and Δ%unfold fall to the right or above the dashed lines, as indicated by the blue arrows

mized their model with sequences from the CALM1_ HUMAN family and calculated fitness scores using the ratio of predicted probabilities for mutant versus wild-type sequences. Their predictions focused on stability scores, not directly predicting T_m or %unfold values.

Team 3: The *Alexov Lab* used the SAAFEC-SEQ method (Li et al. 2021), predicting changes in protein stability ($\Delta\Delta G$) using a gradient boosting decision tree approach. This method considers physicochemical properties, sequence features, and evolutionary conservation. The model was trained on 2,648 mutations from the ProTherm database (Kumar et al. 2006) and further validated. Their predictions centered on protein stability impacts, without directly providing T_m or %unfold values.

Team 4: The *BioSig* team submitted six prediction files using their suite of methods to predict changes in the Gibbs Free Energy of folding ($\Delta\Delta G$). They used structures of CaM from PDB entries 1DMO and 1CLL for the apo and holo forms, respectively. Methods included DUET (Pires et al. 2014a), ENCoM (Frappier et al. 2015), mCSM (Pires et al. 2014b), SDM (Pandurangan et al. 2017), DynaMut (Rodrigues et al. 2018) and DynaMut2 (Rodrigues et al. 2021) to predict $\Delta\Delta G$ and translate them into melting temperature values.

Team 5: The *3BIO-B* team used the HoTMuSiC and Tm-HoTMuSiC methods (Pucci et al. 2016) to predict T_m changes due to single-point mutations. Different structures of CaM were used: PDB structure 1CLL for the holo form and a modeled structure for the apo form obtained with SWISS-MODEL (Waterhouse et al. 2018) and 1DMO as template. They noted a three-state unfolding process for the holo form and provided detailed calculations for %unfold values based on thermodynamic principles.

Team 6: The EASE-MM team employed the EASE-MM method (Folkman et al. 2016), which uses sequence and mutation data to predict protein stability changes ($\Delta\Delta G$) without relying on the protein's 3D structure. This approach used support vector regression models to predict stability changes based on evolutionary conservation, amino acid properties, secondary structure and accessible surface area. They provided T_m and stability score predictions.

Team 7: The *Lichtarge Lab* used the Evolutionary Action (EA) method (Katsonis and Lichtarge 2014), focusing on evolutionary differences among homologous proteins. They combined EA predictions with other tools like MPC (Samocha et al. 2017), PROVEAN (Choi and Chan 2015), MutPred (Mort et al. 2014), and others (see Supplementary Materials), correlating solvent accessibility with %unfold during thermal denaturation. Their model linked %unfold to T_m through linear regression

and submitted predictions based on solvent accessibility calculations for both apo and holo forms.

Team 8: The *Bologna Biocomputing* group utilized the PDB structures 1CFD and 1CLL for Ca^{2+} free and Ca^{2+} bound calmodulin, respectively. They predicted T_m changes using HoTMuSiC (Pucci et al. 2016) and retrieved experimentally validated T_m values from the literature. Stability predictions were based on a consensus score from INPS3D (Savojardo et al. 2016), PoPMuSiC 2.1 (Dehouck et al. 2011), and FoldX (Guerois et al. 2002).

Team 9: The *Strokach* team used four algorithms ELASPIC2 (Strokach et al. 2021), ProteinSolver (Strokach et al. 2020), ProtBert (Elnaggar et al. 2022), and Rosetta (Park et al. 2016) for their predictions. They provided predictions for both the apo and holo forms of calmodulin using both experimental structures and that predicted by AlphaFold (Jumper et al. 2021).

The supplementary materials provide a detailed description of the methods and procedures adopted by each team to predict the impact of the single amino acid substitutions. A comprehensive summary of all submissions is presented in Table S1.

Prediction task and assessment

Participants in the CaM challenge were provided with thermodynamic data for the wild-type calmodulin in both its apo and holo forms. They were asked to predict the melting temperature (T_m) and the percentage of unfolded protein (%unfold) for each variant. Additionally, participants submitted numerical values indicating the impact of each variant on protein stability (*S*). Positive variation of stability corresponds to stabilizing variants, while negative values indicate destabilizing variants.

The predictions of the CaM challenges were assessed considering eight performance measures, comprising five from the regression tasks and three from the classification tasks (section Measures of Performance in Supplementary Materials). We first compared the predicted and experimental values of T_m and %unfold of each protein variant, calculating three types of correlations (Pearson, Spearman and Kendall rank) and two types of errors (Root Mean Square Error and the Mean Absolute Error).

Furthermore, we classified variants as destabilizing or non-destabilizing according to their variation of T_m and %unfold. Variants were classified as destabilizing if their T_m was lower than that of the wild-type ($\Delta T_m = T_m^{mut} - T_m^{wt} < 0.0$ °C). Conversely, variants were considered non-destabilizing if their T_m was equal to or higher than the wild-type ($\Delta T_m = T_m^{mut} - T_m^{wt} \geq 0.0$ °C). Similarly, variants were classified as destabilizing if

they had a higher %unfold compared to the wild-type (Δ%unfold = %unfold^{wt} − %unfold^{mut} < 0.0). Variants were considered non-destabilizing if their %unfold was equal to or lower than that of the wild-type (Δ%unfold = %unfold^{wt} − %unfold^{mut} ≥ 0.0). Using the previous thresholds for the binary classification task, we scored the predictions of the participants considering the predicted impact of the variants (S) by calculating the balanced accuracy (BQ$_2$), the Matthews correlation coefficient (MCC) and the Area Under ROC Curve (AUC).

An important consideration in evaluating predictions is the presence of outliers in the experimental dataset. By "outliers," we refer to experimental measurements that, for various reasons, deviate significantly from the majority of the data. Generally, it is expected that most predictive methods will struggle to accurately predict these outliers. Based on this assumption, our assessment also included evaluating the performance of the algorithms after removing the outliers from the initial CaM challenge dataset. Specifically, for this assessment, we excluded the p.N54I variant from the dataset. This is the only variant located in N-terminal lobe of the CaM structure (Fig. 1) and exhibits different effects on the variation of the T$_m$ values of the apo and holo forms of calmodulin (Fig. 2).

In our assessment, we calculated the average rank across various scores to determine the best predictions. The regression predictions for T$_m$ and %unfold were ranked based on their correlation scores (r_P, r_S, and r_{KT}). Meanwhile, the classification predictions for the variations in protein stability were ranked according to the classification metrics mentioned above (BQ$_2$, MCC, AUC). The performance of each method in predicting the T$_m$, %unfold, and variations in protein stability for both the apo and holo forms of calmodulin was evaluated separately.

The definitions of the eight measures of performance, considered for this assessment, are reported in the supplementary materials. In this assessment, predictions for the variant p.E141G were initially required but later discarded, and predictions for the variant p.F142L were excluded since they were released after the challenge concluded.

Results

Evaluation of predictions for melting temperature and percentage of unfolding

In the first part of our assessment, we evaluated the performance of the participants in predicting the values of the melting temperature (T$_m$) and the percentage of unfolded protein (%unfold) for the apo and holo forms of calmodulin. For T$_m$, the data in Table 3 indicates that the *Strokach*

Table 3 Assessment of the best T$_m$ predictions submitted by each team for the apo and holo forms of calmodulin variants

Apo CaM							
Team	Model	r_P	r_S	r_{KT}	RMSE	MAE	<Rank>
Strokach	5	0.289	0.249	0.185	37.7	36.5	2.0
3billion	2	0.064	0.271	0.185	19.6	18.4	3.7
3BIO-B	1	0.020	− 0.084	− 0.039	2.6	2.1	9.7
BioSig	5	0.080	− 0.068	− 0.126	59.5	59.5	9.7
Lichtarge Lab	6	− 0.119	− 0.161	− 0.068	13.9	10.6	12.7
Bologna Biocomputing	1	− 0.233	− 0.190	− 0.124	4.3	2.6	15.3
EASE-MM	1	− 0.460	− 0.296	− 0.262	59.8	59.8	21.7
Holo CaM							
Team	Model	r_P	r_S	r_{KT}	RMSE	MAE	<Rank>
Strokach	6	0.415	**0.618**	**0.458**	79.8	79.1	3.0
Lichtarge Lab	3	0.481	0.486	0.378	50.7	49.8	3.0
3billion	4	0.491	0.482	0.339	30.0	27.9	3.0
BioSig	5	0.331	0.502	0.378	104.4	104.4	5.0
3BIO-B	1	− 0.645	− 0.079	− 0.070	7.2	4.4	20.7
Bologna Biocomputing	1	− 0.072	− 0.320	− 0.255	6.8	5.2	23.0

Teams were allowed to submit multiple prediction sets using different approaches. The 'Model' column indicates the prediction set that achieved the best performance

r_P, r_S, r_{KT} Pearson, Spearman, Kendall rank, correlation coefficient. *RMSE* Root Mean Square Error, *MAE* Mean Absolute Error, <Rank> The average rank is computed as the mean of the ranks achieved across the three correlation coefficients. In bold are indicated the correlation scores with associated p value below 0.05. The five performance metrics used to evaluate the regression task are defined in the supplementary materials

team submitted the most accurate predictions. The team achieved average correlation coefficients of approximately 0.24 for the apo form and 0.50 for the predictions in holo form of calmodulin. However, significant correlations were observed only for the predictions in Model 6 of the holo form of CaM which were obtained by ELAPSIC2 (Strokach et al. 2021) considering as input the protein structure of the wild-type and mutated proteins predicted with AlphaFold (Jumper et al. 2021). In contrast, for predicting %unfold, the *Lichtarge Lab* provided the best predictions, with average correlation coefficients of 0.57 for the apo form and 0.23 for the holo form of calmodulin (Table 4). Here, significant correlations were observed only for the predictions in Model 4 of the apo form of CaM, which were calculated using a combination of Evolutionary Action (Katsonis and Lichtarge 2014), MPC (Samocha et al. 2017) and the square root of the solvent accessibility. Although the predictions for T_m and %unfold can exhibit significant correlations between experimental and predicted values, they generally display substantial errors, resulting on average in high root mean square error (RMSE) values, with the notable exception of the 3BIO-B team predictions.

Evaluation of the predictions for the impact of variants on protein stability

In the second part of the assessment, we evaluated the performance of each team in predicting the variation in protein stability for each mutant in both the apo and holo forms of calmodulin. This assessment considered changes in melting temperature (ΔT_m) and variations in the percentage of

unfolded protein (Δ%unfold) as indicators of stability. For both metrics, a classification threshold of 0.0 was used. The results for ΔT_m ($T_m^{mut} - T_m^{wt}$) with a threshold of 0.0 °C (Table 5) indicate that the *Alexov Lab* provided the most accurate predictions for the apo CaM, achieving an Area Under the Receiver Operating Characteristic Curve (AUC) of 0.73. However, using a 0.0 °C threshold for classification resulted in lower performance in terms of Balanced Accuracy (BQ_2) and Matthews Correlation Coefficient (MCC). Conversely, the predictions for the stability variation in the holo forms of CaM were significantly more accurate. In this task, teams AIBI-CAGI6, BioSig, and 3BIO-B achieved an AUC of 0.93, with the BioSig team's predictions being particularly outstanding, also showing the highest values in BQ_2 (0.96) and MCC (0.68). The best classification predictions for the effect of CaM protein variants were achieved by the BioSig team in Model 3 by using mCSM (Pires et al. 2014b). On the other hand, when evaluating the predictions using a Δ%unfold (%unfold^{wt} − %unfold^{mut}) threshold of 0.0 (Table 6), the results showed poor performance across all participants. The maximum AUC achieved for predicting the effect of variants on the apo form of CaM was only 0.65.

Evaluation of the performance excluding data outliers

Our dataset includes the p.N54I variant, which is the only variant affecting a residue in the N-terminal lobe of calmodulin. Experimental measurements of T_m indicate that p.N54I impacts on the stability of calmodulin, in both its apo and holo forms, differently from all other variants of the dataset

Table 4 Assessment of the best %unfold predictions submitted by each team for the apo and holo forms of calmodulin variants

Apo CaM							
Team	Model	r_P	r_S	r_{KT}	RMSE	MAE	< Rank >
Lichtarge Lab	4	**0.527**	**0.676**	**0.510**	20.5	18.3	2.3
Strokach	4	− 0.016	0.249	0.202	10.2	7.0	6.7
3BIO-B	2	− 0.336	− 0.444	− 0.329	5.7	4.1	11.0
3billion	1	− 0.595	− 0.472	− 0.337	8.5	7.9	14.0
Holo CaM							
Team	Model	r_P	r_S	r_{KT}	RMSE	MAE	< Rank >
Lichtarge Lab	3	0.277	0.267	0.155	27.9	25.9	1.7
Strokach	2	0.323	0.141	0.058	11.8	9.3	2.0
3billion	2	− 0.068	− 0.149	− 0.097	8.2	7.4	7.0
3BIO-B	2	− 0.381	− 0.102	− 0.077	9.0	7.2	9.0

Teams were allowed to submit multiple prediction sets using different approaches. The 'Model' column indicates the prediction set that achieved the best performance

r_P, r_S, r_{KT} Pearson, Spearman, Kendall rank, correlation coefficient, *RMSE* Root Mean Square Error, *MAE* Mean Absolute Error, < *Rank* > The average rank is computed as the mean of the ranks achieved across the three correlation coefficients. In bold are indicated the correlation scores with associated p value below 0.05. The five performance metrics used to evaluate the regression task are defined in the supplementary materials

Table 5 Evaluation of the best predictions for the variation of stability (S) for both the apo and holo forms of calmodulin variants

Apo CaM

Team	Model	BQ_2	MCC	AUC	$<Rank>$
Alexov Lab	1	0.500	0.000	0.731	3.00
BioSig	6	0.635	0.207	0.385	3.33
3billion	1	0.500	0.000	0.577	3.33
3BIO-B	1	0.615	0.196	0.423	3.67
AIBI-CAGI6	5	0.500	0.000	0.577	3.67
Strokach	4	0.500	0.000	0.558	4.00
Bologna Biocomputing	1	0.346	− 0.237	0.385	7.00
EASE-MM	1	0.115	− 0.555	0.115	11.33

Holo CaM

Team	Model	BQ_2	MCC	AUC	$<Rank>$
BioSig	3	0.964	0.681	0.929	1.00
AIBI-CAGI6	3	0.500	0.000	0.929	4.33
3BIO-B	2	0.500	0.000	0.929	4.33
Bologna Biocomputing	1	0.786	0.286	0.750	4.67
3billion	1	0.500	0.000	0.786	5.00
Strokach	4	0.500	0.000	0.179	6.67
Alexov Lab	1	0.500	0.000	0.071	7.00

Teams were allowed to submit multiple prediction sets using different approaches. The 'Model' column indicates the prediction set that achieved the best performance. The predictions are assessed using a classification threshold for the change in melting temperature (ΔT_m) set at 0.0 °C. $\Delta T_m = T_m^{mut} - T_m^{wt}$

BQ_2 Balanced Accuracy, *MCC* Matthews Correlation Coefficient, *AUC* Area Under the Receiver Operating Characteristic Curve. $<Rank>$ The average rank is computed as the mean of the ranks achieved across the three classification scores. The three performance metrics used to evaluate the classification task are defined in the supplementary materials

(Fig. 2). While most variants tend to leave unaltered, or slightly increase, the stability of the apo form and decrease the stability of the holo form, p.N54I has the opposite effect. Based on this observation, we considered p.N54I as a potential outlier. Consequently, we also evaluated the performance of the methods after excluding this variant from the dataset.

First, we assessed the performance of T_m and %unfold predictions after excluding the p.N54I variant. The results reveal a significant improvement in T_m prediction for the variants of the holo form of calmodulin (Table S2). Specifically, excluding p.N54I, the *Strokach* team's best model achieved a Pearson correlation coefficient of 0.73, which is 0.32 higher than the value obtained considering the entire dataset. In this case, all correlation coefficients (Pearson, Spearman, Kendall rank) between the experimental and predicted values have p-values below 0.05, indicating statistical significance. The regression curves for the best methods, both with and without excluding p.N54I, are shown in Fig. 3. Secondly, we evaluated the performance of the methods in predicting the destabilizing effects of the variants after excluding the p.N54I variant from the dataset. The results show a significant improvement in predicting stability changes for the apo form of calmodulin. Specifically, when

p.N54I was excluded, a binary classifier based on ΔT_m, developed by the *BioSig* team, achieved a BQ_2 score of 0.89, an MCC of 0.44, and an AUC of 0.77 (Table S3). Comparing these results with those from the *Alexov Lab* reveals a modest improvement in AUC (Fig. 4), but more substantial gains in BQ_2 and MCC.

No other significant improvements were observed when comparing other types of predictions. All assessment results for the regression and classification tasks, including both the entire dataset and the dataset excluding the p.N54I variant, are provided in Supplementary File 1 and Supplementary File 2, respectively. All the submissions of the participant to the CAGI6 CaM challenge are provided in Supplementary File 3.

Discussion

In this study, we assessed the predictions submitted for the CAGI6 challenge regarding the impact of amino acid substitutions on the folding process of calmodulin. In detail, for each variant, the participants provided predictions on the melting temperature (T_m), the percentage of unfolded

Table 6 Evaluation of the best predictions for the variation of stability (S) for both the apo and holo forms of calmodulin variants

Apo CaM					
Team	Model	BQ$_2$	MCC	AUC	<Rank>
EASE-MM	1	0.596	0.139	0.596	1.67
AIBI-CAGI6	3	0.500	0.000	0.654	1.67
Alexov Lab	1	0.500	0.000	0.615	2.00
Strokach	4	0.500	0.000	0.442	3.33
3billion	2	0.500	0.000	0.385	4.00
BioSig	5	0.481	− 0.026	0.231	6.00
3BIO-B	2	0.423	− 0.154	0.058	8.00
Bologna Biocomputing	1	0.365	− 0.207	0.288	9.00
Holo CaM					
Team	Model	BQ$_2$	MCC	AUC	<Rank>
BioSig	6	0.527	0.055	0.607	1.67
Alexov Lab	1	0.500	0.000	0.571	4.00
AIBI-CAGI6	3	0.500	0.000	0.482	4.67
Strokach	4	0.500	0.000	0.473	5.00
3billion	3	0.500	0.000	0.446	5.33
3BIO-B	1	0.571	0.286	0.277	6.00
Bologna Biocomputing	1	0.464	− 0.071	0.402	7.33

Teams were allowed to submit multiple prediction sets using different approaches. The 'Model' column indicates the prediction set that achieved the best performance. The predictions are assessed using a classification threshold for the change in the percentage of unfolded protein (Δ%unfold) set at 0.0. $\Delta\%unfold = \%unfold^{wt} - \%unfold^{mut}$

BQ$_2$ Balanced Accuracy, *MCC* Matthews Correlation Coefficient. AUC Area Under the Receiver Operating Characteristic Curve, *<Rank>* The average rank is computed as the mean of the ranks achieved across the three classification scores. The three performance metrics used to evaluate the classification task are defined in the supplementary materials
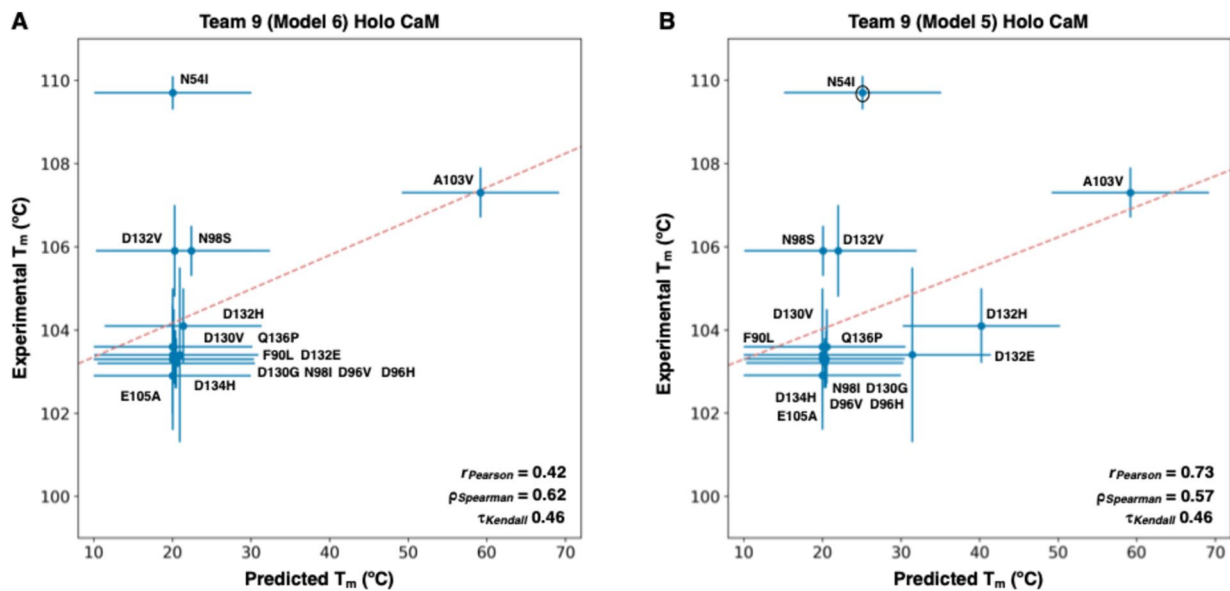
Fig. 3 Regression curves between predicted and experimental T$_m$ values for holo form of calmodulin variants. **A** displays the fitting curve for the best prediction model (model 6) from the *Strokach* team when all variants are included in the assessment. **B** shows the best regression curve (model 5) from the same team when the p.N54I variant was excluded
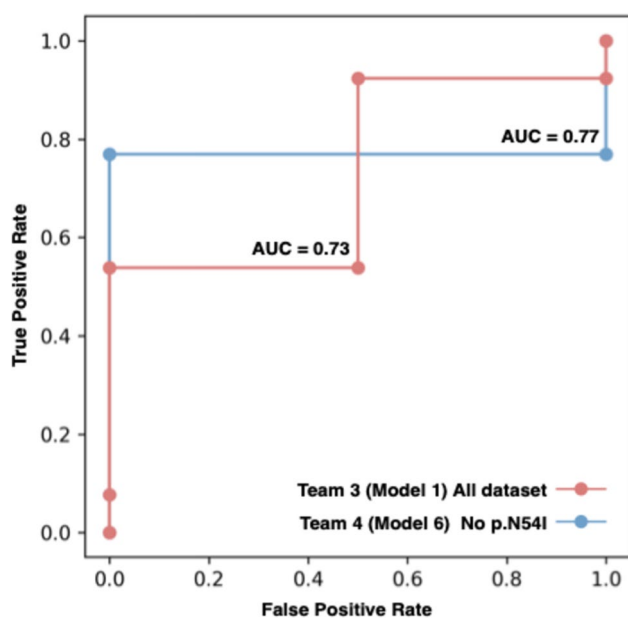
Fig. 4 Comparison of the Receiver Operating Characteristic (ROC) curves for predicting destabilizing variants based on ΔT_m in the apo form. The ROC curve for the *BioSig* team (Team 4) model 6 (blue) was calculated with the p.N54I variant excluded. In contrast, the ROC curve for the *Alexov Lab* (Team 3) model 1 (red) was obtained using the complete set of variants. AUC stands for Area Under the ROC Curve

protein (%unfold) and the impact on protein stability for both the apo and holo forms of calmodulin. The results indicate varying levels of accuracy among participants. For T_m predictions, the *Strokach* team emerged with the highest accuracy, achieving correlation coefficients of approximately 0.50 for holo calmodulin. However, significant correlations were predominantly observed in the holo form. In contrast, predictions for %unfold were most accurately provided by the *Lichtarge Lab*, with correlation coefficients of 0.57 for apo calmodulin. However, none of the teams accurately calibrated their predictions based on wild-type values. In fact, the majority of predictions exhibited relatively high root mean square errors, averaging approximately 36 for T_m and 13 for %unfold.

Moving to the impact of variants on protein stability, the assessment considered changes in T_m (ΔT_m) and %unfold (Δ%unfold). The *Alexov Lab* excelled in predicting ΔT_m for apo calmodulin, achieving an Area Under the Curve (AUC) of 0.73. For holo calmodulin, *AIBI-CAGI6*, *BioSig*, and *3BIO-B* demonstrated very high performance in terms of AUC reaching the value 0.93. However, among them, only the *BioSig* team achieved strong performance in terms of Balanced Accuracy (BQ_2) and Matthews Correlation Coefficient (MCC), scoring values of 0.96 and 0.68, respectively. In contrast, predictions for Δ%unfold

exhibited poorer performance across all participants, with a maximum AUC of only 0.65 for apo calmodulin variants.

An important aspect of the evaluation was the exclusion of the p.N54I variant, identified as an outlier due to its unique impact on calmodulin stability in both apo and holo forms. After excluding that variant, significant improvements were observed in T_m predictions for holo calmodulin, with the *Strokach* team achieving a Pearson correlation coefficient of 0.73. Furthermore, excluding p.N54I led to enhanced predictions of destabilizing effects on apo calmodulin, particularly notable in the performance of the *BioSig* team's binary classifier, which achieved a BQ_2 score of 0.89, MCC of 0.44, and AUC of 0.77.

In summary, while some teams demonstrated good predictive capabilities, particularly in predicting stability changes for calmodulin variants, challenges persisted in accurately predicting real values of T_m and %unfold. It is worth mentioning that the presence of only one mutant in the N-terminal lobe of calmodulin limits the ability to extrapolate the specific roles of each region in the folding process. Moreover, the presence of mutated sites near to the calcium binding sites, or directly involved in the calcium binding itself, may introduce biases in the differences observed between the experimental values obtained for the apo and holo forms of calmodulin. In this context, it is noteworthy that the significantly higher thermal stability of the holo form compared to the apo form implies a crucial role of calcium binding loss in the thermal destabilization observed for most of the mutants analyzed in this study, the majority of which were directly or indirectly involved in calcium binding. However, none of the well-performing prediction methods explicitly accounted for the presence of calcium. This raises the possibility that these methods indirectly "sensed" the presence of calcium e.g. through evolutionary features. However, with the aim of possibly further improving the methods' performance, it could be interesting to test predictors trained on calmodulin-specific datasets or to develop prediction methods that explicitly incorporate the contributions of protein-calcium interactions in their analyses.

Conclusions

The present analysis highlights the effectiveness of combining predictive methods and of utilizing AlphaFold-predicted structures to assess the impact of variants in the CaM protein. Significant correlations were achieved when diverse predictive features, such as evolutionary information, structural properties, and solvent accessibility, were integrated. This suggests that combining alternative approaches, which capture different effects of variants, will enhance prediction accuracy (e.g. Evolutionary Action and MPC). For future challenges, it may be more effective to predict changes in

experimental measures (e.g., T_m and %unfolding) rather than their absolute values, the former resulting in better performance. Additionally, the use of structural models of both wild-type and mutated proteins predicted by Alpha-Fold proved valuable (e.g. AlphaFold structures were used as input of ELAPSIC2 by Strokach team), particularly for tasks relying on structural context, and might prove to be a good practice for other predictors as well. Lastly, adopting a protein-specific training set or developing ligand-aware predictors appear to be promising approaches.

In conclusion, this study highlights the impact of outlier variants on predictive accuracy, emphasizes the importance of selecting a diverse set of variants that comprehensively represent the protein folding process, and suggests some directions for further refinement in computational methods for predicting protein stability.

Declarations

References

Beghi S, Furmanik M, Jaminon A et al (2022) Calcium signalling in heart and vessels: role of calmodulin and downstream calmodulin-dependent protein kinases. Int J Mol Sci 23:16139. https://doi.org/10.3390/ijms232416139

Birolo G, Benevenuta S, Fariselli P et al (2021) Protein stability perturbation contributes to the loss of function in haploinsufficient genes. Front Mol Biosci 8:620793. https://doi.org/10.3389/fmolb.2021.620793

Bohush A, Leśniak W, Weis S, Filipek A (2021) Calmodulin and Its binding proteins in Parkinson's disease. Int J Mol Sci 22:3016. https://doi.org/10.3390/ijms22063016

Chin D, Means AR (2000) Calmodulin: a prototypical calcium sensor. Trends Cell Biol 10:322–328. https://doi.org/10.1016/s0962-8924(00)01800-6

Choi Y, Chan AP (2015) PROVEAN web server: a tool to predict the functional effect of amino acid substitutions and indels. Bioinformatics 31:2745–2747. https://doi.org/10.1093/bioinformatics/btv195

Clapham DE (2007) Calcium signaling. Cell 131:1047–1058. https://doi.org/10.1016/j.cell.2007.11.028

Compiani M, Capriotti E (2013) Computational and theoretical methods for protein folding. Biochemistry 52:8601–8624. https://doi.org/10.1021/bi4001529

Critical Assessment of Genome Interpretation Consortium (2024) CAGI, the critical assessment of genome interpretation, establishes progress and prospects for computational genetic variant interpretation methods. Genome Biol 25:53. https://doi.org/10.1186/s13059-023-03113-6

Crivici A, Ikura M (1995) Molecular and structural basis of target recognition by calmodulin. Annu Rev Biophys Biomol Struct 24:85–116. https://doi.org/10.1146/annurev.bb.24.060195.000505

Dal Cortivo G, Barracchia CG, Marino V et al (2022) Alterations in calmodulin-cardiac ryanodine receptor molecular recognition in congenital arrhythmias. Cell Mol Life Sci 79:127. https://doi.org/10.1007/s00018-022-04165-w

Dal Cortivo G, Marino V, Zamboni D, Dell'Orco D (2023) Impact of calmodulin missense variants associated with congenital arrhythmia on the thermal stability and the degree of unfolding. Hum Genet. https://doi.org/10.1007/s00439-023-02629-y

Dehouck Y, Kwasigroch JM, Gilis D, Rooman M (2011) PoPMuSiC 2.1: a web server for the estimation of protein stability changes upon mutation and sequence optimality. BMC Bioinform 12:151. https://doi.org/10.1186/1471-2105-12-151

Elnaggar A, Heinzinger M, Dallago C et al (2022) ProtTrans: toward understanding the language of life through self-supervised learning. IEEE Trans Pattern Anal Mach Intell 44:7112–7127. https://doi.org/10.1109/TPAMI.2021.3095381

Folkman L, Stantic B, Sattar A, Zhou Y (2016) EASE-MM: sequence-based prediction of mutation-induced stability changes with feature-based multiple models. J Mol Biol 428:1394–1405. https://doi.org/10.1016/j.jmb.2016.01.012

Frappier V, Chartier M, Najmanovich RJ (2015) ENCoM server: exploring protein conformational space and the effect of mutations on protein function and stability. Nucl Acids Res 43:W395-400. https://doi.org/10.1093/nar/gkv343

Gerasimavicius L, Liu X, Marsh JA (2020) Identification of pathogenic missense mutations using protein stability predictors. Sci Rep 10:15387. https://doi.org/10.1038/s41598-020-72404-w

Guerois R, Nielsen JE, Serrano L (2002) Predicting changes in the stability of proteins and protein complexes: a study of more than 1000 mutations. J Mol Biol 320:369–387. https://doi.org/10.1016/s0022-2836(02)00442-4

Hoeflich KP, Ikura M (2002) Calmodulin in action: diversity in target recognition and activation mechanisms. Cell 108:739–742. https://doi.org/10.1016/S0092-8674(02)00682-7

Hussey JW, Limpitikul WB, Dick IE (2023) Calmodulin mutations in human disease. Channels (Austin) 17:2165278. https://doi.org/10.1080/19336950.2023.2165278

Jensen HH, Brohus M, Nyegaard M, Overgaard MT (2018) Human calmodulin mutations. Front Mol Neurosci 11:396. https://doi.org/10.3389/fnmol.2018.00396

Jumper J, Evans R, Pritzel A et al (2021) Highly accurate protein structure prediction with AlphaFold. Nature 596:583–589. https://doi.org/10.1038/s41586-021-03819-2

Karczewski KJ, Francioli LC, Tiao G et al (2020) The mutational constraint spectrum quantified from variation in 141,456 humans. Nature 581:434–443. https://doi.org/10.1038/s41586-020-2308-7

Katsonis P, Lichtarge O (2014) A formal perturbation equation between genotype and phenotype determines the evolutionary action of protein-coding variations on fitness. Genome Res 24:2050–2058. https://doi.org/10.1101/gr.176214.114

Kumar MD, Bava KA, Gromiha MM et al (2006) ProTherm and ProNIT: thermodynamic databases for proteins and protein-nucleic acid interactions. Nucl Acids Res 34:D204-6. https://doi.org/10.1093/nar/gkj103

Landrum MJ, Chitipiralla S, Brown GR et al (2020) ClinVar: improvements to accessing data. Nucl Acids Res 48:D835–D844. https://doi.org/10.1093/nar/gkz972

Li G, Panday SK, Alexov E (2021) SAAFEC-SEQ: a sequence-based method for predicting the effect of single point mutations on protein thermodynamic stability. Int J Mol Sci 22:606. https://doi.org/10.3390/ijms22020606

Linse S, Helmersson A, Forsén S (1991) Calcium binding to calmodulin and its globular domains. J Biol Chem 266:8050–8054. https://doi.org/10.1016/S0021-9258(18)92938-8

Marabotti A, Scafuri B, Facchiano A (2021) Predicting the stability of mutant proteins by computational approaches: an overview. Brief Bioinform 22:bbaa074. https://doi.org/10.1093/bib/bbaa074

Mort M, Sterne-Weiler T, Li B et al (2014) MutPred Splice: machine learning-based prediction of exonic variants that disrupt splicing. Genome Biol 15:R19. https://doi.org/10.1186/gb-2014-15-1-r19

Nussinov R, Wang G, Tsai C-J et al (2017) Calmodulin and PI3K signaling in KRAS cancers. Trends Cancer 3:214–224. https://doi.org/10.1016/j.trecan.2017.01.007

Pancotti C, Benevenuta S, Birolo G et al (2022) Predicting protein stability changes upon single-point mutation: a thorough comparison of the available tools on a new dataset. Brief Bioinform 23:bbab555. https://doi.org/10.1093/bib/bbab555

Pandurangan AP, Ochoa-Montaño B, Ascher DB, Blundell TL (2017) SDM: a server for predicting effects of mutations on protein stability. Nucl Acids Res 45:W229–W235. https://doi.org/10.1093/nar/gkx439

Park H, Bradley P, Greisen P et al (2016) Simultaneous optimization of biomolecular energy functions on features from small molecules and macromolecules. J Chem Theory Comput 12:6201–6212. https://doi.org/10.1021/acs.jctc.6b00819

Petrosino M, Pasquo A, Novak L et al (2019) Characterization of human frataxin missense variants in cancer tissues. Hum Mutat 40:1400–1413. https://doi.org/10.1002/humu.23789

Petrosino M, Novak L, Pasquo A et al (2021) Analysis and interpretation of the impact of missense variants in cancer. Int J Mol Sci 22:5416. https://doi.org/10.3390/ijms22115416

Pires DEV, Ascher DB, Blundell TL (2014a) DUET: a server for predicting effects of mutations on protein stability using an integrated computational approach. Nucl Acids Res 42:W314-319. https://doi.org/10.1093/nar/gku411

Pires DEV, Ascher DB, Blundell TL (2014b) mCSM: predicting the effects of mutations in proteins using graph-based signatures.

Bioinformatics 30:335–342. https://doi.org/10.1093/bioinformatics/btt691

Pucci F, Bourgeas R, Rooman M (2016) Predicting protein thermal stability changes upon point mutations using statistical potentials: introducing HoTMuSiC. Sci Rep 6:23257. https://doi.org/10.1038/srep23257

Radivojac P, Vucetic S, O'Connor TR et al (2006) Calmodulin signaling: analysis and prediction of a disorder-dependent molecular recognition. Proteins 63:398–410. https://doi.org/10.1002/prot.20873

Rodrigues CH, Pires DE, Ascher DB (2018) DynaMut: predicting the impact of mutations on protein conformation, flexibility and stability. Nucl Acids Res 46:W350–W355. https://doi.org/10.1093/nar/gky300

Rodrigues CHM, Pires DEV, Ascher DB (2021) DynaMut2: Assessing changes in stability and flexibility upon single and multiple point missense mutations. Protein Sci 30:60–69. https://doi.org/10.1002/pro.3942

Samocha KE, Kosmicki JA, Karczewski KJ, et al (2017) Regional missense constraint improves variant deleteriousness prediction. bioRxiv. https://doi.org/10.1101/148353

Sanavia T, Birolo G, Montanucci L et al (2020) Limitations and challenges in protein stability prediction upon genome variations: towards future applications in precision medicine. Comput Struct Biotechnol J 18:1968–1979. https://doi.org/10.1016/j.csbj.2020.07.011

Savojardo C, Fariselli P, Martelli PL, Casadio R (2016) INPS-MD: a web server to predict stability of protein variants from sequence and structure. Bioinformatics 32:2542–2544. https://doi.org/10.1093/bioinformatics/btw192

Savojardo C, Petrosino M, Babbi G et al (2019) Evaluating the predictions of the protein stability change upon single amino acid substitutions for the FXN CAGI5 challenge. Hum Mutat 40:1392–1399. https://doi.org/10.1002/humu.23843

Stein A, Fowler DM, Hartmann-Petersen R, Lindorff-Larsen K (2019) Biophysical and mechanistic models for disease-causing protein variants. Trends Biochem Sci 44:575–588. https://doi.org/10.1016/j.tibs.2019.01.003

Strokach A, Becerra D, Corbi-Verge C et al (2020) Fast and flexible protein design using deep graph neural networks. Cell Syst 11:402-411.e4. https://doi.org/10.1016/j.cels.2020.08.016

Strokach A, Lu TY, Kim PM (2021) ELASPIC2 (EL2): combining contextualized language models and graph neural networks to predict effects of mutations. J Mol Biol 433:166810. https://doi.org/10.1016/j.jmb.2021.166810

Sun Y, Shen Y (2024) Structure-informed protein language models are robust predictors for variant effects. Hum Genet. https://doi.org/10.1007/s00439-024-02695-w

Tidow H, Nissen P (2013) Structural diversity of calmodulin binding to its target sites. FEBS J 280:5551–5565. https://doi.org/10.1111/febs.12296

Valeyev NV, Bates DG, Heslop-Harrison P et al (2008) Elucidating the mechanisms of cooperative calcium-calmodulin interactions: a structural systems biology approach. BMC Syst Biol 2:48. https://doi.org/10.1186/1752-0509-2-48

Waterhouse A, Bertoni M, Bienert S et al (2018) SWISS-MODEL: homology modelling of protein structures and complexes. Nucl Acids Res 46:W296–W303. https://doi.org/10.1093/nar/gky427

Won D-G, Kim D-W, Woo J, Lee K (2021) 3Cnet: pathogenicity prediction of human variants using multitask learning with evolutionary constraints. Bioinformatics 37:4626–4634. https://doi.org/10.1093/bioinformatics/btab529

Zhang M, Tanaka T, Ikura M (1995) Calcium-induced conformational transition revealed by the solution structure of apo calmodulin. Nat Struct Biol 2:758–767. https://doi.org/10.1038/nsb0995-758

Zhang J, Kinch LN, Cong Q et al (2019) Assessing predictions on fitness effects of missense variants in calmodulin. Hum Mutat 40:1463–1473. https://doi.org/10.1002/humu.23857

Authors and Affiliations

Paola Turina[1] · Giuditta Dal Cortivo[2] · Carlos A. Enriquez Sandoval[1] · Emil Alexov[3] · David B. Ascher[4,5] · Giulia Babbi[1] · Constantina Bakolitsa[6] · Rita Casadio[1] · Piero Fariselli[7] · Lukas Folkman[8] · Akash Kamandula[9] · Panagiotis Katsonis[10] · Dong Li[11] · Olivier Lichtarge[10] · Pier Luigi Martelli[1] · Shailesh Kumar Panday[3] · Douglas E. V. Pires[12] · Stephanie Portelli[4,5] · Fabrizio Pucci[11] · Carlos H. M. Rodrigues[4] · Marianne Rooman[11] · Castrense Savojardo[1] · Martin Schwersensky[11] · Yang Shen[13] · Alexey V. Strokach[14] · Yuanfei Sun[13] · Junwoo Woo[15] · Predrag Radivojac[9] · Steven E. Brenner[6,16,17] · Daniele Dell'Orco[2] · Emidio Capriotti[1,18]

✉ Daniele Dell'Orco
daniele.dellorco@univr.it

✉ Emidio Capriotti
emidio.capriotti@unibo.it

[1] Department of Pharmacy and Biotechnology, University of Bologna, 40126 Bologna, Italy

[2] Department of Neurosciences, Biomedicine, and Movement Sciences, Section of Biological Chemistry, University of Verona, 37134 Verona, Italy

[3] Department of Physics and Astronomy, Clemson University, Clemson, SC 29634, USA

[4] Computational Biology and Clinical Informatics, Baker Heart and Diabetes Institute, Melbourne, VIC 3004, Australia

[5] School of Chemistry and Molecular Biosciences, Australian Centre for Ecogenomics, University of Queensland, St Lucia, QLD 4072, Australia

[6] Department of Plant and Microbial Biology and Center for Computational Biology, University of California, Berkeley, CA, USA

[7] Department of Medical Sciences, University of Torino, Turin, Italy

[8] Institute for Integrated and Intelligent Systems, Griffith University, Southport, QLD, Australia

[9] Khoury College of Computer Sciences, Northeastern University, Boston, MA 02115, USA

[10] Department of Molecular and Human Genetics, Baylor College of Medicine, Houston, TX, USA

[11] Computational Biology and Bioinformatics, Université Libre de Bruxelles, 50 Roosevelt Ave, 1050 Brussels, Belgium

[12] School of Computing and Information Systems, The University of Melbourne, Melbourne, VIC 3053, Australia

[13] Department of Electrical and Computer Engineering Texas, A&M University, College Station, TX, USA

[14] Department of Computer Science, University of Toronto, Toronto, ON, Canada

[15] 3 Billion, Seoul, South Korea

[16] Biophysics Graduate Group, University of California, Berkeley, CA 94720, USA

[17] Center for Computational Biology, University of California, Berkeley, CA 94720, USA

[18] Computational Genomics Platform, IRCCS University Hospital of Bologna, 40138 Bologna, Italy